Theoretical study of the magnetic x-ray dichroism of Os, Ir, Pt, and Au impurities in Fe

H. Ebert
Research Laboratories (ZFE-ME-TPH11), Siemens A.G., Postfach 3220, D-8520 Erlangen, Federal Republic of Germany

R. Zeller
Institut für Festkörperforschung, Forschungszentrum Jülich, Postfach 1913, D-5170 Jülich, Federal Republic of Germany

(Received 26 February 1990)

The electronic structure of the 5*d* impurities Os, Ir, Pt, and Au in ferromagnetic Fe has been studied by the spin-polarized, relativistic version of the Korringa-Kohn-Rostoker Green's-function method. This approach simultaneously treats spin polarization and spin-orbit coupling and naturally allows for a theoretical investigation of effects arising from an interplay of both. Here the polarization dependence of x-ray absorption (magnetic x-ray dichroism) is considered. For all the impurities studied, the agreement with recent experimental L_2 and L_3 absorption spectra is very satisfactory. For Pt in Fe, a decomposition of the spectra into various absorption channels is presented and the applicability of a simplified model is discussed that interprets the spectra in terms of a spin-polarized band structure alone.

I. INTRODUCTION

Among the various experimental tools probing the local electronic structure, the measurement of the (XANES) x-ray-absorption near-edge structure is a well-established and widely applied method to study the unoccupied electronic states just above the Fermi energy. With the availability of synchrotron radiation with a well-defined polarization, this technique could be refined during the past few years to investigate the absorption spectra with respect to effects caused by the magnetization of the sample.

Using linearly polarized radiation, Sawatzky, Fuggle and co-workers[1] studied the polarization dependence of x-ray-absorption or magnetic x-ray dichroism (MXD) for rare-earth compounds. These authors suggested, however, that more direct information on the magnetism of a system could be obtained by using circularly polarized radiation. This technique, adopted by Schütz and coworkers,[2] has now applied to a large number of rare-earth and transition-metal systems.[2–4] While for most of the rare-earth compounds an atomic description seems to be applicable, the itinerant-electron picture of magnetism is without doubt the adequate one when transition metals are concerned. Based on the itinerant-electron picture we have developed a first-principles theory of the MXD of transition metals by using the spin polarized relativistic version of the Korringa-Kohn-Rostoker Green's-function method to describe the electronic structure of the system.[5] In our theory we are able to treat spin-orbit coupling and spin polarization on an equal footing. The interplay of both effects is—just as for the more familiar magneto-optical Kerr effect (MOKE)—the fundamental source of the MXD. A brief outline of our formalism, which we first applied to pure Fe,[5] is given in Sec. II. A generalization to treat impurity systems is straightforward and the first results for Pt in Fe have already been published elsewhere.[6] In Sec. III A we present the theoretical L_2 and L_3 spectra for Os, Ir, Pt, and Au and discuss these spectra in comparison with recent experimental data. A decomposition of the theoretical spectra into individual absorption channels allows for a detailed interpretation of the spectra as we demonstrate for Pt in Fe (Sec. III B). Our treatment of spin-orbit coupling and spin polarization on the same level is not perturbational. Thus, in principle, no restrictions exist for the applicability to the calculation of the MXD, but obviously this treatment does not allow for an easy description of the spectra in familiar terms as, for example, densities of states for spin-up or spin-down electrons. Such a description has been developed in a model by Schütz *et al.*[2,4] In their model the effect of spin-orbit coupling is taken into account by an electron-polarization parameter P_e. This allow them to deduce the relative difference in the density of states for spin-up and spin-down electrons from the experimental absorption spectra. In Sec. III B we give a detailed discussion of whether the model picture of Schütz *et al.* can be justified on the basis of our rigorous approach.

II. THEORETICAL FRAMEWORK

As mentioned above, XANES is a well-established tool used to study the local electronic structure of multicomponent systems. Accordingly, theoretical descriptions of XANES have been developed by various authors.[7] Among these the formulation given by Durham[8] for studying the interaction of electrons with an electromagnetic radiation field seems to be particularly powerful. This formulation is based on the multiple-scattering theory to ensure a realistic one-particle description of the electronic structure and is applicable to pure systems and dilute alloys as well as to ordered or disordered compounds with the same rigor.

Quite generally the absorption coefficient μ measured in a XANES experiment is proportional to the sum over quantum-mechanical transition rates

$$\mu \sim \sum_i W_i^{q\lambda}(\omega) , \tag{1}$$

where $W_i^{q\lambda}$ describes the probability that the absorption of a photon of wave vector $\mathbf{q}$, polarization λ, and energy $\hbar\omega$ induces a transition from a core state i into the unoccupied conduction-band states.

Originally Durham's expression for $W_i^{q\lambda}(\omega)$ was written down in a nonrelativistic form. Its relativistic counterpart is given by

$$\begin{aligned} W_i^{q\lambda}(\omega) = -\frac{1}{\Gamma} \int d^3r \int d^3r' \, \phi_i^x(\mathbf{r}) X_{q\lambda}(\mathbf{r}) \\ \times \mathrm{Im} G^+(\mathbf{r},\mathbf{r}', E_i+\hbar\omega) \\ \times X_{q\lambda}^x(\mathbf{r}') \phi_i(\mathbf{r}') \\ \times \Theta(E_i+\hbar\omega-E_F) , \end{aligned} \tag{2}$$

where the interaction vertex $X_{q\lambda}$ has the form

$$X_{q\lambda}(\mathbf{r}) = -e\underline{\boldsymbol{\alpha}} \cdot \mathbf{A}(\mathbf{r}) = -e\underline{\boldsymbol{\alpha}} \cdot \mathbf{a}_\lambda e^{i(\mathbf{q}\cdot\mathbf{r}+\omega t)} + \mathrm{H.c.} \tag{3}$$

Here $\underline{\boldsymbol{\alpha}}$ is the vector of the standard Dirac matrices and $\mathbf{A}(\mathbf{r})$ represents the vector potential corresponding to the x-ray photons, with its amplitude vector $\mathbf{a}_\lambda$ perpendicular to the photon wave vector $\mathbf{q}$. The polarization λ of the photons is expressed by the vector $\mathbf{a}_\lambda$, where we use the convention that $\mathbf{a}_\lambda = a_\lambda(1,i,0)$ stands for left and $\mathbf{a}_\lambda = a_\lambda(1,-i,0)$ for right circularly polarized light if $\mathbf{q}$ points along the z axis (0,0,1). In (2) the core wave functions for the initial state are described by Dirac spinors $\phi_i(\mathbf{r})$, the manifold of final states is described by the one-electron Green's function for the Dirac equation, and the step function Θ guarantees that only unoccupied conduction-band states can be reached. Within the spin-polarized relativistic multiple-scattering theory[9] $G^+(\mathbf{r},\mathbf{r}',E)$ can be written as

$$\begin{aligned} G^+(\mathbf{r},\mathbf{r}',E) = \sum_{\Lambda\Lambda'} Z_\Lambda(\mathbf{r},E) \tau_{\Lambda\Lambda'}^{nn}(E) Z_{\Lambda'}^x(\mathbf{r}',E) \\ - \sum_\Lambda Z_\Lambda(\mathbf{r}_<,E) J_\Lambda^x(\mathbf{r}_>,E) , \end{aligned} \tag{4}$$

where Λ stands for the pair of relativistic quantum numbers (κ,μ). Z_Λ (J_Λ) is the regular (nonregular) scattering solution of the single-site Dirac equation for a spin-dependent potential, and $\tau_{\Lambda\Lambda'}^{nn}(E)$ the site diagonal scattering path operator. Equations (3) and (4) can be used in (2) to rewrite the transition rate $W_i^{q\lambda}$ in the form

$$\begin{aligned} W_i^{q\lambda} = -\frac{1}{\Gamma} \sum_{\Lambda,\Lambda'} M_\Lambda^i(E_i+\hbar\omega) \mathrm{Im} \tau_{\Lambda\Lambda'}^{nn}(E_i+\hbar\omega) \\ \times M_{\Lambda'}^{i*}(E_i+\hbar\omega) , \end{aligned} \tag{5}$$

where the matrix elements $M_\Lambda^i(E)$ are given by

$$\begin{aligned} M_\Lambda^i(E) &= \mathrm{Tr} \int d^3r \, \phi_i^x(\mathbf{r}) (-e\underline{\boldsymbol{\alpha}} \cdot \mathbf{a}_\lambda) e^{i\mathbf{q}\cdot\mathbf{r}} Z_\Lambda(\mathbf{r},E) \\ &= \mathrm{Tr} \int d^3r \, \phi_i^x(\mathbf{r}) (-e\underline{\boldsymbol{\alpha}} \cdot \mathbf{a}_\lambda) \\ &\quad \times (1 + i\mathbf{q}\cdot\mathbf{r} + \cdots) Z_\Lambda(\mathbf{r},E) . \end{aligned} \tag{6}$$

The first term in the expansion of the exponential function in (6) of course describes the electric dipole approximation, whereas the next terms describe the magnetic dipole, electric quadrupole contributions, etc.

The evaluation of the matrix elements M_Λ^i is more complicated than in the nonrelativistic case since in general the functions ϕ_i and Z_Λ have no unique spin-angular character.[9,10] This effect arises from the spin-dependent potential $V(\mathbf{r})$ describing the spin polarization of the system. The spin-dependent part of the $V(\mathbf{r})$ couples partial waves with the same μ value and parity and the wave functions Z_Λ generally have the form

$$Z_\Lambda(\mathbf{r},E) = \sum_{\Lambda'} Z_{\Lambda'\Lambda}(\mathbf{r},E) \tag{7}$$

with

$$Z_{\Lambda'\Lambda}(\mathbf{r},E) = \begin{pmatrix} g_{\Lambda'\Lambda}(r,E) \chi_{\Lambda'}(\hat{\mathbf{r}}) \\ i f_{\Lambda'\Lambda}(r,E) \chi_{-\Lambda'}(\hat{\mathbf{r}}) \end{pmatrix} , \tag{8}$$

where $-\Lambda$ stands for $(-\kappa,\mu)$.

The first index Λ' of $Z_{\Lambda'\Lambda}$ describes its spin-angular character and the second index Λ the asymptotic behavior of the function Z_Λ. For a given Λ, the various large and small components, $g_{\Lambda'\Lambda}$ and $f_{\Lambda'\Lambda}$ satisfy a set of coupled radial Dirac equations.

Writing the core wave functions ϕ_i analogously to (7) leads, for the matrix elements, to

$$\begin{aligned} M_\Lambda^i(E) = ie \sum \int dr \, r^2 g_{\Lambda_i'\Lambda_i}(r,E_i) f_{\Lambda'\Lambda}(r,E) A_{\Lambda_i'-\Lambda'}^\lambda \\ - \int dr \, r^2 f_{\Lambda_i'\Lambda_i}(r,E_i) g_{\Lambda'\Lambda}(r,E) A_{-\Lambda_i'\Lambda'}^\lambda . \end{aligned} \tag{9}$$

The angular part $A_{\Lambda_i'\Lambda'}^\lambda$ is given by products of Clebsch-Gordan coefficients as

$$\begin{aligned} A_{\Lambda\Lambda'}^+ &= 2C(l\tfrac{1}{2}j;\mu-\tfrac{1}{2},+\tfrac{1}{2}) C(l'\tfrac{1}{2}j';\mu'+\tfrac{1}{2},-\tfrac{1}{2}) \\ &\quad \times \delta_{ll'}\delta_{\mu'-\mu,+1} , \\ A_{\Lambda\Lambda'}^- &= 2C(l\tfrac{1}{2}j;\mu+\tfrac{1}{2},-\tfrac{1}{2}) C(l'\tfrac{1}{2}j';\mu'-\tfrac{1}{2},+\tfrac{1}{2}) \\ &\quad \times \delta_{ll'}\delta_{\mu'-\mu,-1} \end{aligned} \tag{10}$$

for left ($\lambda=+$) and right ($\lambda=-$) circularly polarized light if only electric dipole transitions are used. The quantum numbers $\Lambda=(\kappa,\mu)$ and j are connected by the relation $j=|\kappa|-\frac{1}{2}$. Equation (10) obviously fixes the selection rules for the excitation process in the dipole approximation as $l-l'=\pm1$ and $\mu'-\mu=\pm1$ depending on the helicity of the radiation. For the higher dipole-forbidden contributions expressions analogously to (9) and (10) and the corresponding selection rules can be found in a straightforward manner.

Expression (9) for the matrix elements can be simplified by neglecting the usually small contributions from the coupling of partial waves with the different l values. Thus, the summations in (9) can be restricted to $\Lambda'=\bar{\Lambda},\Lambda$ and $\Lambda_i'=\bar{\Lambda}_i,\Lambda_i$ with $\bar{\Lambda}=(-\kappa-1,\mu)$. If only s core states are involved in the absorption process the initial wave functions have unique spin-angular character and one simply has $\Lambda_i'\equiv\Lambda_i$. This is not the case for the L_2 and

L_3 spectra, where the initial states are $2p_{1/2}$ and $2p_{3/2}$ core states. Because of the spin-dependent potential the substates of the shells, which can still be labeled by the magnetic quantum number μ, possess some admixed $p_{3/2}$ or $p_{1/2}$ character corresponding to $\Lambda_i' = \bar{\Lambda}_i$. Furthermore these substates degenerate in the paramagnetic case are generally split in energy. In our present calculations for the $5d$ elements in Fe this splitting and admixture of $\bar{\Lambda}$ character turned out to be very small for the $2p$ states. For this reason, we could ignore these effects of the spin-dependent potential in the calculations of the spectra presented in Sec. III. Whereas this approximation is justified for the systems studied here, it is, however, doubtful for atoms with a large magnetic moment and if core states are studied with higher principal quantum numbers.

The multiple-scattering theory we use to describe the electronic structure of the investigated systems gives the above formalism a very powerful flexibility as detailed below. The matrix elements M_i^{Λ} in (5) vary smoothly with energy and depend only on the atomic potential $V(\mathbf{r})$ on the selected crystal site. This is easily seen from (6) because the matrix elements are directly determined by the single-site solutions Z_{Λ} and the core wave functions ϕ_i. All the information on the geometry and configuration of the system is contained in the scattering path operator $\tau^{nn}_{\Lambda\Lambda'}$, which essentially determines the energetical structure of the absorption spectra. For pure systems the scattering path operator $\tau^{nn}_{\Lambda\Lambda'}$ is calculated by a Brillouin-zone (BZ) integral

$$\tau^{nn}_{\Lambda\Lambda'}(E) = \frac{1}{\Omega_{\mathrm{BZ}}} \int_{\mathrm{BZ}} d^3k [t^{-1}(E) - G(\mathbf{k},E)]^{-1}_{\Lambda\Lambda'} . \quad (11)$$

Here t stands for the on-the-energy-shell single-site t matrix and G is the relativistic form for the matrix of Korringa-Kohn-Rostoker (KKR) structure constants $G_{\Lambda\Lambda'}(\mathbf{k},E)$. Numerical details concerning the evaluation of the Brillouin-zone integral in (11) can be found, for example, in Ref. 9. For ordered multicomponent systems it is straightforward to generalize (11). In that case the index n of the scattering operator specifies both the unit cell and atomic type. For impurity systems the situation is more complicated because the translation symmetry is broken. Here the use of multiple-scattering theory has the advantage that the corresponding impurity projected scattering path operator can be obtained from a simple algebraic relation

$$\tau^{nn}_{\mathrm{imp}} = \tau^{nn}_{\mathrm{host}} [1 - (t^{-1}_{\mathrm{host}} - t^{1}_{\mathrm{imp}}) \tau^{nn}_{\mathrm{host}}]^{-1} . \quad (12)$$

This form of (12) is valid if potential perturbations of neighboring host atoms are neglected. It represents the single-site approximation and is sufficient for our present calculations. Finally, for a disordered system the component projected scattering path operator is obtained within the formalism of the Soven-Taylor coherent-potential approximation (CPA) from an expression similar to (12) where the host specific quantities are replaced by those representing the CPA effective medium.

The results presented below are based on self-consistent Hohenberg-Kohn-Sham local-density-functional calculations of the potentials for the $5d$ elements in Fe.[11] The calculations have been performed in a scalar-relativistic way accounting for all relativistic effects apart from spin-orbit coupling. For the present purpose it is sufficient to include perturbations on the next-nearest-neighbor Fe atoms of the impurity for calculating the potential and to use the single-site approximation in the last fully relativistic iteration for obtaining the impurity scattering path operator τ^{nn}_{imp} via (11).

III. RESULTS AND DISCUSSION

A. Comparison with experiment

The MXD of late $5d$ transition metals in Fe has recently been measured by Schütz *et al.*[4] using the transmission technique and in the case of Pt in Fe also by the fluorescence technique.[12] The spectra resulting from the transmission experiments at the L_2 and L_3 absorption edges of Os, Ir, Pt, and Au are shown in Figs. 1(a)–1(d) for left and right circularly polarized x rays. The most prominent feature in these spectra is the peak at the absorption edge. These so-called white lines are more pronounced for the L_3 than for the L_2 spectra. Assuming that the L_2 and L_3 spectra more or less exclusively arise from the unoccupied $d_{3/2}$ and $d_{5/2}$ bands (see below), this simply reflects the fact that the impurity states at higher energies should primarily be of $d_{5/2}$ character. With increasing atomic number the dominance of the white lines is reduced for Au they nearly vanish. The spectra shown in Figs. 1(a)–1(d) are very similar to those of the corresponding pure $5d$ transition metals. For the pure systems the white lines reflect the unoccupied part of a rather broad d band, which has normally a width of 7–10 eV. In the case of $5d$ impurities the white lines arise from virtual bound-state-like densities of states with a prominent peak centered close to the Fermi level. With increasing attractivity of the potential this peak is successively filled and shifts towards higher binding energies.

The pronounced polarization dependence of the various spectra can already be seen in Figs. 1(a)–1(d). It is exhibited more clearly by plotting the relative difference in absorption for left and right circularly polarized radiation: $R = (\mu^+ - \mu^-)/(\mu^+ + \mu^-)$ [Figs. 2(a)–2(d)]. For all the $5d$ transition-metal impurities in Fe the maximum of $|R|$ is of the order of 10%. Even for Au in Fe the maximum of $|R|$ reaches 5% and for L_2 edge of Pt in Fe $|R|$ exceeds 20%, which is the highest value found until now. These values are much higher than the maxima of R found for the K absorption edges of the pure transition metals Fe, Co, and Ni, where it reaches only 0.5%. As mentioned above, the MXD has its origin—just as the MOKE—in the interplay of the spin polarization and spin-orbit coupling. For this reason R should roughly scale with the local spin moment and the spin-orbit coupling strength. Because of the relatively small spin moments of Os, Ir, Pt, and Au in Fe one would expect that the MXD is reduced compared to the pure $3d$ metals. On the other hand, the increase of the spin-orbit coupling with the atomic number should lead to an enhanced MXD for the $5d$ elements. In order to distinguish be-

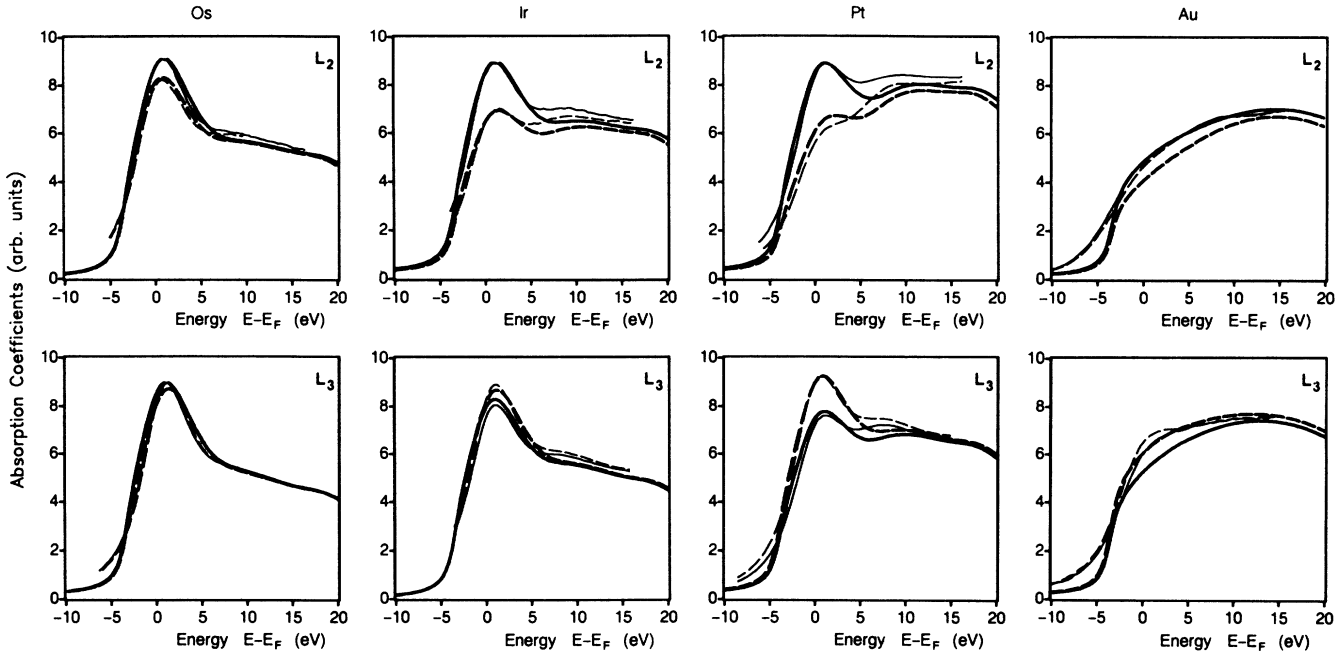

FIG. 1. Absorption coefficients μ for left and right circularly polarized x rays for the L_2 and L_3 edges of Os, Ir, Pt, and Au in Fe. Thick (thin) lines mark theoretical (experimental) results and solid (dashed) lines are for left (right) circularly polarized x-ray radiation.

tween the influence of local spin moments and spin-orbit coupling strengths it is however, not justified to compare R for the $L_{2,3}$ edges of $5d$ elements in Fe with R for the K edges of the $3d$ metals because they are caused by quite different processes.

The MXD at the K edges of the $3d$ elements is caused only by spin-orbit coupling of the $4p$ conduction-band states and the (negligible) spin polarization of the initial $1s$ core states. In contrast to this rather simple situation the MXD at the $L_{2,3}$ edges of the $5d$ atoms in Fe is also determined by spin-orbit coupling of the initial $2p$ core states. More meaningful is, therefore, a comparison of the $3d$ K spectra with K or L_1 spectra of the $5d$ atoms in Fe. The L_1 edge of Pt in Fe shows a MXD effect similar to that for the K edge of Fe.[13] In both cases the maximum is nearly equally large. Consequently the 12 times smaller spin moment of Pt compared to Fe is roughly compensated by the increased spin-orbit coupling arising from the higher atomic number.

A striking difference between the R values for the L_2

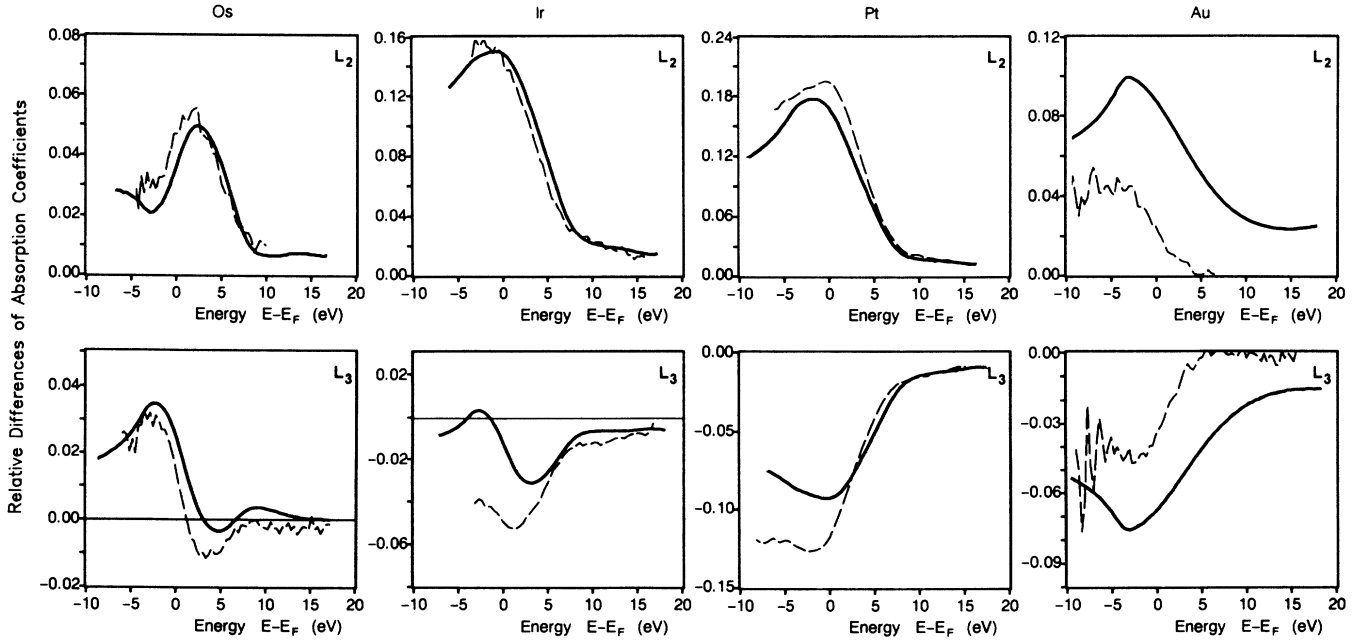

FIG. 2. Relative differences R of the absorption coefficients between left and right circularly polarized x rays for the L_2 and L_3 edges of Os, Ir, Pt, and Au in Fe. Thick lines are for the theoretical and thin lines for the experimental results.

and L_3 spectra is the opposite sign in these curves for Ir, Pt, and Au. It is a straightforward to explain this result in the model developed by Schütz *et al.*[2,4] to describe the MXD of transition metals. In analogy to the Fano effect for free atoms,[14] these authors assume that an effective polarization P_e of the electron arises when it is excited by circularly polarized light from a full shell into a spin-orbit split final state. For cubic symmetry the corresponding absorption coefficient for left and right circularly polarized light only differ in spin-polarized systems. Electrons with polarization $+P_e$ and $-P_e$ fit with different probabilities into the bands with spin-up and spin-down polarization and lead to different absorption coefficients. The model of Schütz *et al.* artificially divides the absorption process into two steps: the excitation including the polarization of the electron and the settling in the final state. For the first step it is not unreasonable to borrow the parameter P_e from calculations for free atoms as done in Refs. 2 and 12. The calculations show that L_2 spectra should consist nearly exclusively of $2p_{1/2} \rightarrow 5d_{3/2}$ transitions, while the $2p_{3/2} \rightarrow 5d_{5/2}$ transitions are primarily ($\sim 90\%$) responsible for the L_3 spectra. The corresponding P_e values have a ratio of around $-2{:}1$ and therefore explain the opposite sign of R for the L_2 and L_3 spectra.

According to the model of Schütz *et al.* the experimental R_L values (which they call μ_c/μ_0), if divided by P_e, give the relative difference for spin-up and spin-down polarization in the l projected density of states, with l determined by the dipole-selection rules. This procedure has been used by Schütz *et al.* to compare their experimental spectra with results of (scalar-relativistic) band-structure calculations. In the case of the Fe K edge reasonable agreement has been found.[2] For the L_3 spectra of the late $5d$ elements in Fe the corresponding agreement was also astonishingly good.[4] This is not true for the L_2 spectra. In the model one would expect that for the L_2 and L_3 edges R/P_e values *both* correspond to the same relative spin polarization of the unoccupied calculated d conduction band. As Figs. 2(a)–2(d) show this is not the case for the L_2 spectra, a particularly striking discrepancy is found for Os in Fe. In contrast to the model of Schütz *et al.* the fully relativistic treatment of the x-ray absorption process for spin polarized systems as outlined in Sec. II treats the electronic excitation in one step and includes the effects of spin polarization and spin-orbit coupling simultaneously. The resulting spectra are shown in Figs. 1(a)–1(d).

For the comparison with the experiments the calculated curves have been broadened to account for various broadening mechanisms. The spectra have been folded with Lorentzians (as in Ref. 15) to describe the finite lifetimes of the core hole and excited electrons and to take the experimental resolution into account. As can be seen, in (almost) all cases very satisfying agreement between theoretical and experimental absorption coefficients is obtained. In the case of Au experimental problems seem to exist which lead to an extraordinarily poor experimental resolution.[13] Instead of a comparison of the μ_L^{λ} curves it is more instructive to compare the corresponding R curves [shown in Figs. 2(a)–2(d)]. Again a very satisfying agreement is found clearly demonstrating that our theoretical approach is able to reproduce all the features in the experimental spectra—even in a quantitative way. Furthermore, obviously no problems exist to deal with the L_2 spectra including the case of Os, which was not described by the model of Schütz *et al.*

From the overall good agreement it is reasonable to conclude that the results of the electronic structure calculations represent a good description for charge and magnetization densities of Os, Ir, Pt, and Au atoms in Fe. Thus the MXD experiments as local probes confirm the antiferromagnetic coupling of the Os spin moment to the Fe host magnetization. This is in contradiction to the interpretation of early neutron-scattering experiments[16] (being much less local probes) in terms of a ferromagnetic Os spin moment.

B. Model of Schütz *et al.*

In this section we give a more detailed analysis of our calculated $L_{2,3}$ spectra for Pt in Fe and discuss to which extent the model of Schütz *et al.* can be justified on the basis of our results. In particular, we want to study the three main assumptions of the model. First, can L_2 or L_3 edges be described exclusively by $2p_{1/2} \rightarrow 5d_{3/2}$ or $2p_{3/2} \rightarrow 5d_{5/2}$ transitions, respectively. Secondly, can the concept of κ-projected, spin-polarized densities of states be used separately for $d_{3/2}$ and $d_{5/2}$ empty states. Thirdly, does the absorption of circularly polarized x rays produce an energy-independent amount P_e of spin-polarized electrons. To answer these questions we have performed a detailed analysis of (5) for the particular case of Pt in Fe. We also compare this $5d$ impurity atom with the pure $3d$ element Fe.

Equation (5) clearly shows that a unique decomposition with respect to angular quantum numbers j or κ is impossible and that cross terms arise. Their importance can be seen from Fig. 3 for the L_2 and L_3 edges for left circularly polarized x-rays (+) of Pt in Fe (for right circular polarization the results are rather similar). For the L_2 edge the total absorption is very well represented by summing the transitions $2p_{1/2} \rightarrow 5d_{3/2}$, $2p_{1/2} \rightarrow 6s_{1/2}$, and neglecting the cross terms. For that, e.g., the partial spectrum $2p_{1/2} \rightarrow 5d_{3/2}$ has been obtained by summing only terms for $\tau^{nn}_{+2\mu,+2\mu}$, i.e., $j = j' = \frac{3}{2}$. This procedure does not completely suppress the $d_{5/2}$ contribution in a rigorous sense since the wave functions contain Z_{Λ} partial waves with $d_{5/2}$ character. From Fig. 3 it can be seen that over the shown energy range of 25 eV the $2p_{1/2} \rightarrow 5d_{3/2}$ transition gives the dominant contribution to the total absorption spectrum with considerably more than 90%. For the L_3 edge the situation is not so clear. Particularly near the absorption edge the cross terms contribute to a certain extent. The relative contributions of the $2p_{3/2} \rightarrow 5d_{5/2}$, $2p_{3/2} \rightarrow 5d_{3/2}$, and $2p_{3/2} \rightarrow 6s_{1/2}$ transitions for the L_3 edge show a stronger energy variation than the corresponding transitions for the L_2 edge. However, it is still justified to consider the $2p_{3/2} \rightarrow 5d_{5/2}$ transition as the dominant one with around 90% intensity, whereas the $2p_{3/2} \rightarrow 5d_{3/2}$ and $2p_{3/2} \rightarrow 6s_{1/2}$ transitions contribute around 5–10%, respectively. This

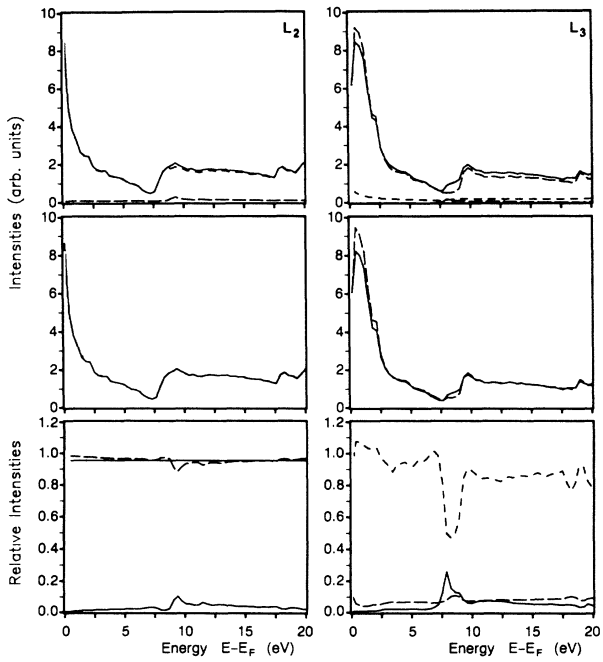

FIG. 3. Diagonal contributions for the L_2^+ (excitation of $p_{1/2}$ core states) and L_3^+ (excitation of $p_{3/2}$ core states) absorption spectra of Pt in Fe. The upper panel contains the contributions of $p_{1/2}\rightarrow s_{1/2}$ (long-dashed line) and $p_{1/2}\rightarrow d_{3/2}$ (short-dashed line) transitions for the L_2^+ spectrum and of $p_{3/2}\rightarrow d_{3/2}$ (long-dashed line) and $p_{3/2}\rightarrow d_{5/2}$ (short-dashed line) transitions for the L_3^+ spectrum and their respective sums (solid lines). The middle panel shows these sums (dashed lines) compared to the exact results (solid lines). The lower panel shows the relative contributions of $p_{1/2}\rightarrow s_{1/2}$ (solid line) and $p_{1/2}\rightarrow d_{3/2}$ (dashed line) transitions for the L_2^+ edge and of $p_{3/2}\rightarrow s_{1/2}$ (solid line), $p_{3/2}\rightarrow d_{3/2}$ (long-dashed line), and $p_{3/2}\rightarrow d_{5/2}$ (short-dashed line) transitions for the L_3^+ edge.

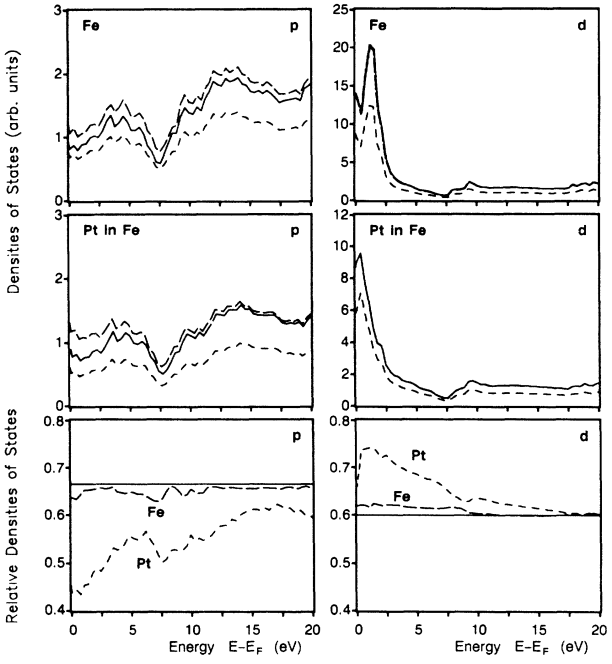

FIG. 4. Left and right sides show p- and d-projected local densities of states for Fe (upper panel) and Pt in Fe (middle panel). On the left side $p_{3/2}$ (short-dashed lines), the sum of $p_{1/2}$ and $p_{3/2}$ (long-dashed line) and the total p contribution (solid lines) are given. On the right side $d_{5/2}$ (short-dashed lines), the sum of $d_{3/2}$ and $d_{5/2}$ (long-dashed lines) and the total d contribution (solid lines) are given. The lower panel shows the relative values of $n_{p_{3/2}}/(n_{p_{1/2}}+n_{p_{3/2}})$ and $n_{d_{5/2}}/(n_{d_{3/2}}+n_{d_{5/2}})$ local densities of states.

analysis obviously shows that the first assumption in the model of Schütz *et al.* is reasonably valid, the L_2 edges essentially arise from $2p_{1/2}\rightarrow 5d_{3/2}$ transitions and the L_3 edges mainly from $2p_{3/2}\rightarrow 5d_{5/2}$ transitions.

For the second assumption we first examine the concept of a κ-projected density of states and then its extension to the spin-polarized case. In Fig. 4 we show the total p-projected densities of states in comparison with the results obtained by summing only terms diagonal in κ. For both considered systems, Pt in Fe and pure Fe, it is seen that for higher energies the summation of diagonal $p_{1/2}$ and $p_{3/2}$ contributions is sufficient to represent the total p-projected densities of states showing that cross terms are small in that energy range. For lower energies, however, considerable discrepancies occur. Moreover for Pt in Fe it is not true that $p_{1/2}$ and $p_{3/2}$ states contribute with the ratio 1:2 as it is the case for pure Fe where the small spin-orbit coupling nearly leads to a value $n_{p_{3/2}}/(n_{p_{1/2}}+n_{p_{3/2}})=\frac{2}{3}$. In the case of Pt in Fe the $p_{1/2}$ density of states is considerably too large and $n_{p_{3/2}}/(n_{p_{1/2}}+n_{p_{3/2}})$ is smaller than $\frac{2}{3}$. This is in full agreement with results of Nemoshkalenko *et al.*[17] for all the pure $5d$ metals. These authors also find a contribution of $6p_{1/2}$ states much larger than corresponding to a ratio 1:2. The concept of a κ-projected density of states is, therefore, only of restricted validity for the p states. Contrary to that the concept can be used for d states as Fig. 4 shows. The sum of $d_{3/2}$- and $d_{5/2}$-projected densities of states agrees very well with the exact results, cross terms can clearly be neglected. For pure Fe, similar to the p-projected densities of states, the ratio $n_{d_{5/2}}/(n_{d_{3/2}}+n_{d_{5/2}})$ differs only slightly from $\frac{3}{5}$ which would occur for vanishing spin-orbit coupling. On the other hand, for Pt in Fe the $d_{5/2}$ diagonal density of states contributes clearly more than $\frac{3}{5}$. This naturally arises because the upper unoccupied part of the Pt d band contains more $d_{5/2}$ character, whereas the lower occupied part contains more $d_{3/2}$ character (see also Ref. 17). Our results for the other $5d$ elements dissolved in Fe are very similar to those of Fig. 4 for Pt in Fe. Consequently, the concept of κ-projected densities of states is rather well justified for these systems. On the other hand, the concept of a κ-projected spin polarization seems to be rather useless as Fig. 5 shows both for pure Fe and Pt in Fe. The results are obtained by suppressing as above all nondiagonal terms in the evaluation of

$$m(E)=-\frac{1}{\pi}\mathrm{Tr}\,\mathrm{Im}\beta\sigma_z G(\mathbf{r},\mathbf{r},E)\ . \tag{13}$$

The structure of the sums of $d_{3/2}$- and $d_{5/2}$-projected spin polarizations are similar to the exact results which include all cross terms, but considerable discrepancies ex-

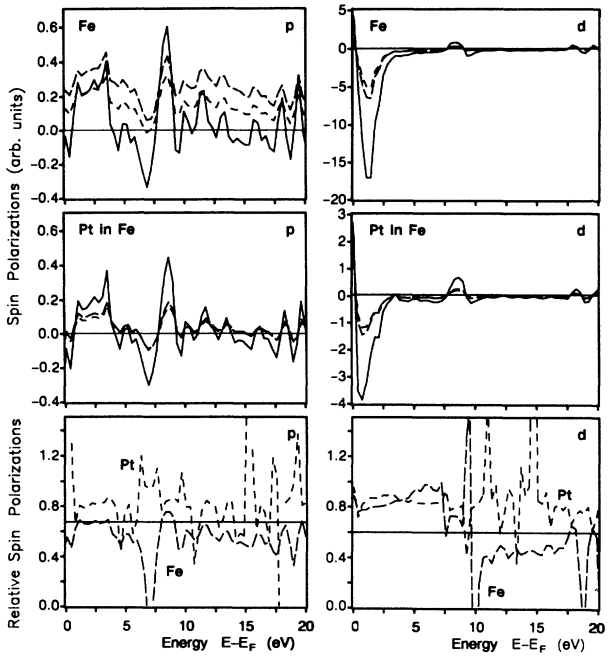

FIG. 5. Left and right sides show p- and d-projected local spin polarizations for Fe (upper panel) and Pt in Fe (middle panel). The lower panel shows the relative values of $m_{p_{3/2}}/(m_{p_{1/2}}+m_{p_{3/2}})$ and $m_{d_{5/2}}/(m_{d_{3/2}}+m_{d_{5/2}})$ local spin polarizations. The meaning of the lines is analogous to Fig. 4.

ist for the magnitude. Only about 50% of the total spin polarization can be attributed to $d_{3/2}$ and $d_{5/2}$ diagonal terms clearly showing that the notion of κ-projected spin polarization can be applied only with caution. Particularly striking is the fact that the $d_{3/2}$ contribution is much smaller than the $d_{5/2}$ contribution. This certainly arises because a projection on $d_{5/2}$ subbands is strictly possible for $\mu=\pm\frac{5}{2}$. These subbands contain no admixture of $d_{3/2}$ character and possess pure spin character $\langle\sigma_z\rangle=\pm1$. The different behavior of $d_{3/2}$- and $d_{5/2}$-projected spin polarizations obviously also influences the amount of spin polarization relative to the density of states (Fig. 6). For the $d_{3/2}$ part it is 70–90% smaller than for the total d band, whereas the $d_{5/2}$ part only deviates by 40–60%. These discrepancies again show that it is not possible to talk about a spin polarization of a

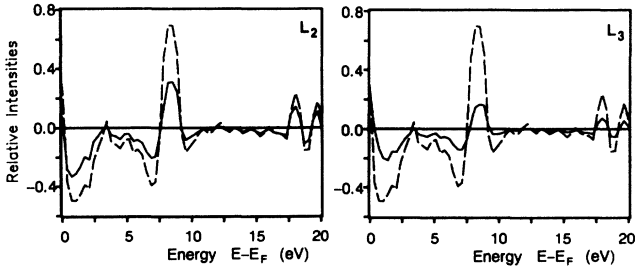

FIG. 6. Relative differences R of the calculated absorption coefficients for the L_2 and L_3 edges of Pt in Fe (solid lines) compared to the relative local spin polarizations m_d/n_d (dashed lines) for the Pt d band in Fe.

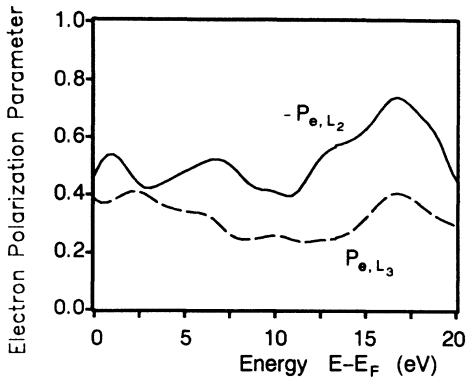

FIG. 7. Calculated energy-dependent electron polarization parameters $P_e=(m_d/n_d)/R$ for the L_2 and L_3 absorption edges of Pt in Fe. (The curves have been somewhat smoothed.)

$d_{3/2}$ or $d_{5/2}$ subband. Nevertheless, for the here considered cases of 5d impurity atoms in Fe a substantial contribution arises from $d_{5/2}$ character. The $d_{3/2}$ contribution is rather small and the rest arises from cross terms. From this result it is at least partly plausible that the experimentally derived[4] relative spin polarizations m_d/n_d agree much better with the band-structure calculations for the L_3 spectra than for the L_2 spectra.

From these results we also conclude that theoretical results for the electron polarization parameter P_e cannot be derived by comparing calculated R values with the corresponding calculated κ-projected relative spin-polarization curves $m_{d_{3/2}}/n_{d_{3/2}}$ and $m_{d_{5/2}}/n_{d_{5/2}}$. Instead it seems to be more reasonable to compare the R values for the L_2 and L_3 edges with the calculated total relative spin polarization m_d/n_d. As Fig. 7 shows a relatively slightly energy-dependent polarization parameter P_e is obtained. It agrees rather well with atomic calculations which yield $P_e\approx-0.5$ for the Pt L_2 edge and $P_e\approx-0.25$ for the L_3 edge. In spite of the above explained restrictions this good agreement confirms the idea of an energy-independent parameter P_e on which the model of Schütz *et al.* is based.

IV. CONCLUSION

We have presented a rigorous relativistic formalism to describe the x-ray dichroism of magnetic materials (MXD). Its reliability and flexibility has been demonstrated by calculating the MXD spectra of the late 5d transition metals dissolved as impurities in Fe. We have found excellent agreement between our calculation and the available experimental data. This fact establishes our formalism as a useful tool for future detailed and quantitative interpretations of MXD spectra. One disadvantage of our present approach is the large computational effort inherent in the spin-polarized relativistic KKR method, especially for systems with a big unit cell. As will be shown in a forthcoming publication,[18] this numerical effort can easily be reduced substantially. Another problem, obvious from Sec. II, is that our approach does not allow straightforward interpretation of the MXD spectra in terms of quantities which are familiar from scalar—or

nonrelativistic band-structure calculations. However, as we have demonstrated, our formalism can be used to examine the usefulness of simpler models as, e.g., that of Schütz *et al.* In particular, it was possible to investigate the various assumptions in this simplified two-step model. We found that this model contains the essential aspects of MXD spectra for the considered systems because the electron polarization parameter deduced from atomic calculations remains more or less unchanged in the solid-state environment. Nevertheless, it is rather clear that the experimentally derived spin polarization cannot be interpreted as the one of κ-projected subbands. For the systems we investigated it is rather the spin polarization of the total d band. Since the scalar-relativistically calculated spin polarization agrees reasonably well with the fully relativistically calculated one, we conclude that it is justified for most systems to use the spin-polarized scalar-relativistic calculations to interpret the experimental spectra.

ACKNOWLEDGMENTS

We like to thank G. Schütz for valuable discussions and B. Drittler for the preparation of the self-consistent impurity potentials.

[1]B. T. Thole, G. van der Laan, and G. A. Sawatzky, Phys. Rev. Lett. **55**, 2086 (1985); G. van der Laan, B. T. Thole, G. A. Sawatzky, J. B. Goedkoop, J. C. Fuggle, J.-M. Esteva, R. Karnatak, J. P. Remeika, and H. A. Dabkowska, Phys. Rev. B **34**, 6529 (1986); J. B. Goedkoop, B. T. Thole, G. van der Laan, G. A. Sawatzky, F. M. F. de Groot, and J. C. Fuggle, *ibid.* **37**, 2086 (1988).

[2]G. Schütz, W. Wagner, W. Wilhelm, P. Kienle, R. Zeller, R. Frahm, and G. Materlik, Phys. Rev. Lett. **58**, 737 (1987).

[3]G. Schütz, M. Knülle, R. Wienke, W. Wilhelm, W. Wagner, P. Kienle, and R. Frahm, Z. Phys. B **73**, 67 (1988).

[4]G. Schütz, R. Wienke, W. Wilhelm, W. Wagner, P. Kienle, R. Zeller, and R. Frahm, Z. Phys. B **75**, 495 (1989).

[5]H. Ebert, P. Strange, and B. L. Gyorffy, J. Appl. Phys. **63**, 3055 (1988); Z. Phys. B **73**, 77 (1988).

[6]H. Ebert, B. Drittler, R. Zeller, and G. Schütz, Solid State Commun. **69**, 485 (1989); H. Ebert and R. Zeller, Physica B (Amsterdam) **161**, 191 (1989).

[7]See, for example, *Synchrotron Radiation Research,* edited by H. Winich and S. Doniach (Plenum, New York, 1980).

[8]P. J. Durham, in *The Electronic Structure of Complex Systems,* edited by P. Phariseau and W. M. Temmerman (Plenum, New York, 1984).

[9]P. Strange, H. Ebert, J. B. Staunton, and B. L. Gyorffy, J. Phys. Condens. Matter **1**, 2959 (1989).

[10]P. Strange, J. B. Staunton, and B. L. Gyorffy, J. Phys. C **17**, 3355 (1984).

[11]For details, see B. Drittler, N. Stefanou, S. Blügel, R. Zeller, and P. H. Dederichs, Phys. Rev. B **40**, 8203 (1989), and references therein.

[12]G. Schütz and R. Wienke, Hyperfine Interact. **50**, 457 (1989).

[13]G. Schütz (private communication).

[14]U. Fano, Phys. Rev. **178**, 131 (1968); **184**, 250 (1969).

[15]J. E. Müller, O. Jepsen, and J. W. Wilkins, Solid State Commun. **42**, 365 (1982).

[16]M. F. Collins and G. G. Low, Proc. Phys. Soc. **86**, 535 (1965); I. A. Campbell, *ibid.* **89**, 71 (1966); J. Phys. C **1**, 687 (1968).

[17]V. V. Nemoshkalenko, V. N. Antonov, Vl. N. Antonov, W. John, H. Wonn, and P. Ziesche, Phys. Status Solidi B **111**, 11 (1982).

[18]H. Ebert (unpublished).